Morphology-Aware HRV Estimation from Wrist PPG in Sedentary Scenarios

Changshuo Hu*
Singapore Management University
cs.hu.2023@phdcs.smu.edu.sg

Hung Manh Pham*
Singapore Management University
hm.pham.2023@phdcs.smu.edu.sg

Dong Ma†
Singapore Management University
dongma@smu.edu.sg

ABSTRACT

Photoplethysmography (PPG) is widely used in wearable devices for non-invasive heart rate variability (HRV) monitoring. While most prior work focuses on mitigating motion artifacts, recent studies highlight that even subtle contact pressure variations can distort waveform morphology and lead to inaccurate HRV estimates. In this work, we propose a morphology-aware deep learning framework that conditions HRV estimation on beat-level waveform types. Our model jointly encodes the raw PPG waveform and a sequence of pressure-induced morphology labels using parallel encoders, integrates them via cross-attention, and predicts normal-to-normal (NN) intervals and beat count to support downstream HRV computation. Evaluated on the public WF-PPG dataset, our method significantly improves estimation accuracy over pressure-agnostic baselines and narrows the gap toward clean finger PPG references.

1 INTRODUCTION

Photoplethysmography (PPG) is a common optical technique used in both clinical and wearable devices, ranging from finger-clip monitors [20] to smartwatches [6], and earbuds [5]. By emitting light into the skin and measuring the reflected or transmitted signal, PPG captures pulsatile changes in blood volume and supports the estimation of various physiological parameters, such as heart rate, heart rate variability (HRV), oxygen saturation, and diseases like arterial stiffness and atrial fibrillation [1]. Among these, HRV is particularly valuable as a non-invasive marker of autonomic nervous system activity, with broad applications in stress detection [13], fatigue monitoring [14], and cardiovascular health [29].

HRV refers to the beat-to-beat variability in heart rhythm [2], typically computed from the sequence of normal-to-normal (NN) intervals rather than simply measuring the variance of heart rate. Standard HRV metrics, such as the Root Mean Square of Successive Differences (RMSSD), are derived from temporal fluctuations between consecutive systolic peaks [3], waveform onsets [8], or valleys [30]. Unlike other physiological indicators such as heart rate or blood oxygen saturation, which can be derived from relatively coarse signal features, HRV estimation requires accurately locating fiducial points across successive pulse cycles. As a result, HRV is highly sensitive to waveform morphology, and even subtle signal distortions can lead to erroneous interval estimation.

Prior research on reliable HRV estimation primarily focuses on addressing motion artifacts using signal processing [25], deep learning [4, 15], or auxiliary sensors such as inertial measurement units (IMUs) [17]. However, as highlighted in recent research[10], even under sedentary conditions, variations in contact pressure between the PPG sensor and the skin can affect tissue compression and blood perfusion. These changes lead to morphological distortions in the PPG waveform, such as amplitude suppression, baseline shifts, and the loss of diastolic components. Consequently, the NN intervals become highly variable, resulting in inaccurate HRV estimation.

In this work, inspired by the observation that pressure-induced morphological changes in PPG waveforms are closely associated with shifts in beat positions, we hypothesize that explicitly modeling waveform morphology can help disambiguate distorted NN intervals and enable more accurate HRV estimation. Rather than recovering an ideal waveform or relying solely on raw signal features, we propose a morphology-guided deep learning framework that conditions HRV estimation on beat-level waveform types. Our system jointly processes two information streams derived from the same wrist PPG signal: the raw waveform and a symbolic sequence of waveform types that reflect beat-wise morphological distortion. The architecture consists of a morphology-aware PPG encoder and a lightweight waveform type encoder, each extracting complementary features from the input segment. These features are fused via a cross-attention module that aligns physiological and distortion-related cues. The fused representation is decoded into an NN interval sequence and a beat count estimate, supporting downstream computation of standard HRV metrics.

We train and evaluate our model on a public PPG dataset, WF-PPG [10], which provides synchronized wrist PPG and ECG signals collected under systematically varied contact pressures. Experimental results show that our approach significantly outperforms pressure-agnostic baselines and narrows the gap toward clean PPG references. In summary, this work presents and demonstrates the effectiveness of a morphology-aware deep learning framework for robust HRV estimation under varying contact pressure in sedentary conditions.

2 PRELIMINARY

PPG is a non-invasive optical technique that measures blood volume changes in peripheral vessels. It works by shining light from an LED into the skin and measuring the amount of light either absorbed or reflected by the underlying tissue, which varies with pulsatile

*Co-primary authors.
†Corresponding author.

UbiComp Companion '25, October 12–16, 2025, Espoo, Finland

ACM ISBN 979-8-4007-1477-1/2025/10…$15.00
https://doi.org/10.1145/3714394.3756171

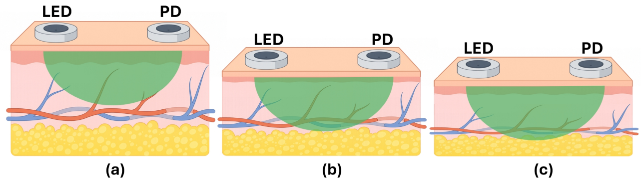

Figure 1: Reflective PPG sensing under different contact pressures. The LED emits light into the skin, and the photodiode (PD) captures the reflected signal. (a) Low pressure: light interacts with shallow capillaries. (b) Moderate pressure: light reaches deeper arteries. (c) High pressure: excessive compression reduces perfusion and distorts the signal.

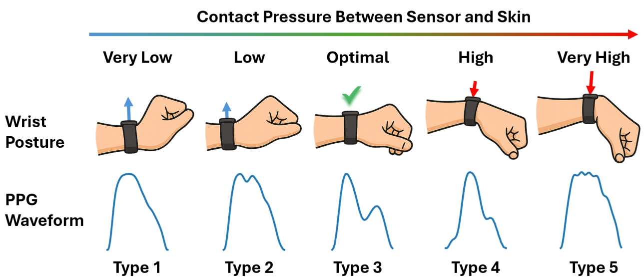

Figure 2: Variations in PPG waveforms induced by contact pressure changes under different wrist postures.

blood flow. In wearable devices such as smartwatches, a reflective PPG configuration is typically used, where both the light source and the photodetector are placed on the same surface of the skin.

PPG waveform morphology is highly sensitive to practical use conditions. In particular, contact pressure (e.g., the tightness of a smartwatch) affects both the physiological state of the skin and the optical path through which light interacts with blood vessels. When the pressure is low as Figure 1(a), the skin remains relaxed and the light primarily interacts with shallow capillaries, yielding low-amplitude signals [16, 22]. At moderate pressure as Figure 1(b), compression of soft tissue allows the light to reach deeper arteries with stronger pulsatile flow, resulting in more pronounced waveforms [28]. Under excessive pressure as Figure 1(c), superficial vessels collapse and local perfusion decreases, distorting the optical path and degrading signal morphology. These pressure-induced changes affect both the amplitude and temporal structure of the reflected signal, even in the absence of motion.

Figure 2 presents examples of wrist PPG waveform morphologies under varying contact pressures induced by different wrist postures. As shown, each pressure level produces a characteristic waveform shape, ranging from delayed low-intensity signals to flattened waveforms with suppressed diastolic features. These morphology shifts have a direct impact on downstream tasks such as HRV estimation. Metrics like the Root Mean Square of Successive Differences (RMSSD) and the Standard Deviation of Normal-to-Normal intervals (SDNN) rely on consistent detection of fiducial points such as the systolic peak, onset, or valley. When the waveform shape is distorted, peak detection becomes unreliable, resulting in jitter,

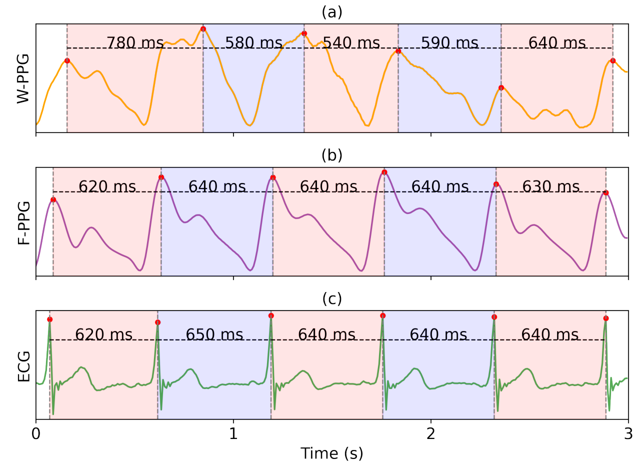

Figure 3: Example of synchronized (a) wrist PPG, (b) finger PPG, and (c) ECG signals from the WF-PPG dataset. While finger PPG and ECG exhibit consistent NN intervals, wrist PPG shows irregularities due to contact pressure variations.

missed beats, or false positives, which in turn compromises the accuracy of HRV estimation.

To further illustrate this problem, we extract synchronized wrist PPG (under varying contact pressure), finger PPG (under consistent optimal contact pressure), and ECG signals (ground truth) from the public WF-PPG dataset [10] under a prolonged sitting condition. As shown in Figure 3, finger PPG shows consistent peak-to-peak intervals that closely match the ECG ground truth. In contrast, wrist PPG exhibits noticeable distortions and irregular peak locations due to subtle variations in contact pressure. These distortions compromise the reliability of peak detection, making accurate HRV estimation challenging. This highlights the need for a more advanced HRV estimation approach that can robustly handle waveform distortions induced by contact pressure variations.

3 SYSTEM DESIGN

3.1 Overview

We present a morphology-aware deep learning framework for robust estimation of heart rate variability (HRV) from wrist-worn PPG signals, which are often distorted due to varying contact pressures. Figure 4 illustrates the overall architecture. Given a 60-second wrist PPG segment, the system first performs beat segmentation and waveform classification to assign each beat a canonical morphology label, reflecting pressure-induced distortion types (labeled 1–5 in the WF-PPG dataset). The raw PPG waveform and the derived waveform type sequence are then processed by two parallel encoders: a morphology-aware PPG encoder and a symbolic waveform encoder. Their outputs are fused via a cross-attention mechanism, allowing the model to jointly reason about the correlation between signal structure and distortion patterns. The resulting fused representation is decoded into a sequence of NN intervals along with an estimated beat count. The estimated beat count is used to determine the number of valid intervals within the predicted sequence, which are then used for deriving HRV metrics.

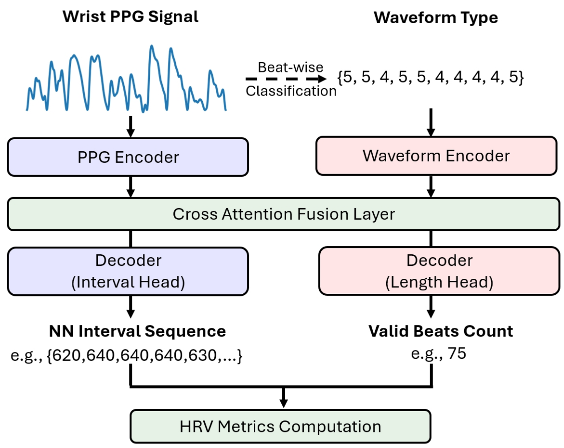

Figure 4: Overview of the proposed framework, which takes a wrist PPG signal and its derived waveform type sequence as input, and outputs the NN interval sequence and beat count for HRV computation.

3.2 Segmentation and Classification

Our framework leverages beat-level annotations with waveform type labels provided by the WF-PPG dataset, where each heartbeat is categorized into one of five canonical morphology types reflecting different levels of pressure-induced distortion (as illustrated in Figure 2). During inference, we replicate this process by applying the same segmentation and classification pipeline used in the dataset to derive the waveform type sequence. Specifically, we classify waveform morphologies into five types based on the timing of the systolic peak, the presence of a diastolic peak, and the relative magnitudes of the two peaks. For example, Type 1 includes only the systolic peak, whereas Type 2 contains both systolic and diastolic peaks with comparable magnitudes. As shown in Figure 3(a), these waveform types capture significant morphological variations caused by different contact pressure levels and provide valuable context for interpreting the underlying PPG dynamics. We use the waveform type sequence to inform the model of beat-wise signal quality, enabling more accurate and robust HRV estimation.

3.3 PPG Encoder

To capture fine-grained physiological dynamics from raw PPG signals, we adopt a morphology-aware encoder inspired by the PAPAGEI framework [23], which has demonstrated strong generalization across diverse PPG-related tasks. Pre-trained on over 57,000 hours of PPG data using morphology-aware contrastive learning and mixture-of-experts objectives, PAPAGEI is designed to extract robust representations under varying signal conditions. Our encoder closely follows its core architecture: a ResNet-style 1D convolutional network comprising 18 residual blocks with progressively increasing channel widths. Each block integrates grouped convolutions, batch normalization, ReLU activations, and dropout layers. Given a fixed-length input segment, the encoder outputs a 512-dimensional embedding that summarizes key morphological and rhythmic features. With approximately 5 million parameters, the encoder strikes a balance between representation capacity and computational efficiency, making it well-suited for deployment in resource-constrained settings such as mobile health applications.

3.4 Waveform Encoder

While raw pressure signals can offer valuable information about signal distortion, they are rarely available on commercial devices and would require additional sensors and integration effort. Instead, we leverage a symbolic sequence of waveform types derived directly from the PPG signal through beat-level classification. These waveform types, labeled from Type 1 to Type 5 in the WF-PPG dataset, reflect varying levels of pressure-induced morphological distortion and provide a compact, interpretable representation of signal quality over time.

To leverage this information, we introduce a waveform encoder that processes the type sequence to complement the morphology-aware PPG embedding. The input to this encoder is a sequence of waveform-type labels, corresponding to individual heartbeats in a 60-second window under resting conditions [1]. The sequence is embedded into a learnable vector space, then passed through two fully connected layers with SiLU activations. The first layer expands the embedded sequence to a 256-dimensional intermediate representation, and the second projects it to a 512-dimensional output embedding. The resulting embedding is subsequently fused with the PPG encoder output to enable distortion-aware HRV estimation.

3.5 Cross-Attention Fusion Layer

To effectively combine the information encoded in the PPG waveform and the waveform type sequence, we adopt a lightweight cross-attention mechanism. This design enables each embedding stream to attend to salient features in the other, facilitating contextual reasoning between morphology and distortion cues while improving robustness under signal degradation. We implement two single-head cross-attention blocks in a symmetric configuration: in the first block, the PPG embedding acts as the query and the waveform embedding as the key-value source; in the second block, their roles are reversed. Each block projects the inputs into a common latent space before computing scaled dot-product attention, followed by context-aware feature aggregation. The outputs of the two attention blocks are averaged to form a fused 512-dimensional representation, which captures interactions between the two streams and is passed to the decoding stage for HRV estimation.

3.6 Decoder

The fused representation produced by the cross-attention module is passed to two decoding heads that jointly support HRV estimation: an interval head and a length head. Rather than predicting aggregated HRV metrics directly, our design estimates the underlying NN interval sequence, enabling flexible and fine-grained downstream analysis.

[1] We fix the sequence length to 180, as the typical human heart rate ranges from 60 to 180 beats per minute. For input segments with fewer heartbeats, we apply zero-padding to reach the desired length.

Interval Head. The primary decoding head performs sequence regression to estimate the NN intervals in milliseconds. Each element in the output sequence (with a length of 180) corresponds to the time gap between two successive heartbeats.

Length Head. The auxiliary head outputs a scalar indicating the number of valid NN intervals within the input and output segments. This predicted length is used to dynamically mask invalid elements during both training and inference, ensuring that loss computation and performance evaluation are based only on meaningful outputs. It also acts as an implicit quality indicator for the interval predictions.

Loss Function. The overall training loss is a weighted sum of the interval regression loss and the length prediction loss. We empirically set the weights to $\lambda_1 = 0.6$ and $\lambda_2 = 0.4$ to prioritize accurate interval estimation while still guiding the model to predict the correct number of intervals:

$$\mathcal{L} = \lambda_1 \cdot \mathcal{MSE}_{\text{interval}} + \lambda_2 \cdot \mathcal{MSE}_{\text{length}} \tag{1}$$

4 DATASET DESCRIPTION

4.1 WF-PPG Dataset

We conduct our study using WF-PPG [10], a publicly available dataset specifically designed to examine the effects of contact pressure on PPG waveform morphology. The dataset includes recordings from 27 healthy participants, each undergoing six seated sessions in a controlled environment. During each session, wrist PPG signals were collected under five systematically varied contact pressure levels using a custom clamp mechanism with real-time pressure measurement. Simultaneously, fingertip PPG was recorded under stable, optimal pressure to serve as a clean reference. In addition, ECG signals were captured using a chest-worn sensor to provide ground-truth heartbeat timings for HR and HRV calculation. All signals, wrist PPG, reference finger PPG, and ground truth ECG, were synchronized across modalities through a combination of hardware triggers and signal-based alignment. Each wrist PPG waveform is labeled into one of five morphology types, reflecting progressive distortions caused by increasing pressure. Each participant contributed approximately 24 minutes of synchronized data, with PPG signals originally sampled at 128 Hz and ECG at 130 Hz. In the released version, both signals were resampled to 100 Hz and the PPG cycles were annotated with different types based on the developed algorithm.

4.2 Preprocessing

To prepare the data for training and evaluation, we adopt a subject-independent partitioning strategy. Specifically, we allocate 18 participants to the training set, 4 to the validation set, and 5 to the test set (27 in total). This ensures that all test subjects are entirely unseen during training, allowing us to evaluate generalizability to new users without requiring subject-specific calibration. No user identity or demographic information was used during training. Each segment is 60 seconds long and extracted using a sliding window with a 3-second stride, resulting in 4,463 training segments, 1,305 validation segments, and 1,891 test segments.

We use the synchronized wrist PPG and ECG signals provided in the WF-PPG dataset. The wrist PPG and waveform type serve as the primary input for model training, while ECG provides ground truth heartbeat timings for computing target HRV metrics. The dataset includes finger PPG signals recorded under optimal contact pressure, serving as a reference for the best signal quality and performance that PPG can achieve. So we also use the finger PPG in our experiment.

5 PERFORMANCE EVALUATION

5.1 HRV Evaluation Metrics

To evaluate our system's ability to estimate HRV, we compare the predicted values of each HRV metric against ECG-derived ground truth and report the mean absolute error (MAE). We focus on a set of standard indices that reflect different aspects of cardiac rhythm dynamics. These metrics are computed from predicted NN intervals and include:

- **Standard Deviation of NN intervals (SDNN)** quantifies the overall variability in heart rate across the entire recording. It is computed as the standard deviation of all NN intervals and serves as a general indicator of autonomic balance.
- **Root Mean Square of Successive Differences (RMSSD)** measures short-term variability between successive heartbeats. It is calculated as the square root of the mean squared differences between adjacent NN intervals and reflects rapid fluctuations in heart rate.
- **pNN20** is the percentage of successive NN interval pairs that differ by more than 20 ms. It reflects the frequency of large beat-to-beat changes and is associated with parasympathetic modulation.
- **SD1** is a geometric index derived from the Poincaré plot, representing the standard deviation perpendicular to the line of identity. It captures short-term HRV and is mathematically related to RMSSD.
- **High-Frequency Power (HF, 0.15–0.4 Hz)** represents the spectral power of high-frequency heart rate oscillations derived from NN intervals. It is commonly linked to respiration-related parasympathetic activity.

5.2 Overall Performance

Table 1 presents a comparative analysis of HRV estimation errors under three conditions: (1) wrist PPG without waveform type conditioning, (2) wrist PPG with conditioning (our proposed method), and (3) finger PPG under optimal pressure as a clean reference. Across all five HRV metrics, our method consistently reduces the mean absolute error (MAE) compared to the unconditioned baseline.

The last row of the table reports the percentage of the error gap between wrist and finger PPG, which is closed by our method. Notably, the gap is closed by 93.85% in SD1, 80.95% in SDNN, and 68.14% in pNN20, indicating that waveform type conditioning significantly enhances the robustness of HRV estimation under pressure-induced distortions. While the absolute MAE reductions may appear modest, it is important to note that our method already approaches the performance ceiling defined by high-quality finger PPG. Given the limited room for further improvement, these results underscore the effectiveness and convergence of our approach. Moreover, since even finger PPG is subject to physiological variability and sensor noise, the remaining error likely reflects an irreducible floor rather than correctable model bias.

Table 1: Mean absolute errors (MAEs) of HRV metrics.

Method	SDNN	RMSSD	pNN20	SD1	HF
Wrist PPG (No Type)	0.0098	0.0082	10.191	0.0156	0.0126
Finger PPG (Reference)	0.0077	0.0047	8.1370	0.0091	0.0101
Wrist PPG (With Type)	**0.0081**	**0.0069**	**8.7915**	**0.0095**	**0.0117**
Gap Closed (%)	80.95	37.14	68.14	93.85	36.00

Table 2: Impact of cross-attention fusion.

Method	SDNN	RMSSD	pNN20	SD1	HF
Feature Concatenation	0.0083	0.0096	9.6567	0.0102	0.0182
Cross-Attention Fusion	**0.0081**	**0.0069**	**8.7915**	**0.0095**	**0.0117**

5.3 Effect of Cross-Attention Fusion

To further validate the effectiveness of our design, we conduct an ablation study by replacing the cross-attention fusion module with a simple feature concatenation and merging strategy. The results are shown in Table 2. Across all five HRV metrics, the model with cross-attention fusion consistently achieves lower estimation errors. In particular, RMSSD error drops from 0.0096 to 0.0069, SD1 decreases from 0.0102 to 0.0095, and HF improves notably from 0.0182 to 0.0117. These results suggest that enabling strong, structured inter-branch communication between the PPG encoder and the waveform type encoder is crucial for effectively leveraging supportive type information in pressure-distorted HRV estimation.

6 RELATED WORK

In this section, we review prior work on two areas: how contact pressure affects PPG signal characteristics, and how HRV is estimated from PPG under various signal conditions.

6.1 PPG and Contact Pressure

Recent studies have systematically examined how contact pressure between the skin and the PPG sensor alters signal characteristics. Due to the soft, deformable nature of human tissue, varying pressure levels cause different degrees of compression, which in turn modify the path and intensity of light propagation. These changes affect both the amplitude and morphology of the PPG waveform.

May et al. [16], using phantom models and controlled experimental setups, demonstrated that variations in contact pressure can cause substantial changes in waveform amplitude and morphology. Subsequent studies [22, 28] further revealed that there exists an optimal pressure range that yields the highest signal quality. Beyond signal morphology, contact pressure-induced distortions also reduce the accuracy of physiological indices such as heart rate [26] and blood pressure [7]. However, most prior work stops at characterizing these effects, without explicitly modeling contact pressure or proposing practical strategies to mitigate its impact. As a result, pressure-induced variability is often treated as random noise rather than a structured and controllable factor.

To support more systematic investigations, the WF-PPG dataset [10] explicitly introduces contact pressure as a controlled variable. It provides wrist PPG signals collected under five discrete pressure levels, along with synchronized finger PPG and ECG ground truth. In this work, we leverage this dataset as the foundation for developing a learning-based framework that accounts for contact pressure during model training and inference for reliable HRV estimation.

6.2 HRV Estimation

HRV refers to temporal fluctuations between successive heartbeats, typically quantified using NN intervals. It is widely used as a non-invasive proxy for autonomic nervous system activity and is associated with states such as stress [13], fatigue [14], and cardiovascular health [29]. While standard HRV estimation relies on ECG-based R-peak detection, alternative modalities such as PPG, camera-based remote PPG [12], microphone-based acoustic sensing [18], and radar [9] have been explored to enable wearable and unobtrusive monitoring. Among these, PPG is particularly popular due to its low cost, compact form factor, and ease of integration.

PPG-based HRV estimation typically involves detecting fiducial points such as the systolic peak [3], valley [8], or waveform onset [30] to derive NN intervals. Traditional pipelines rely on filtering and peak detection [3], while recent deep learning methods infer HRV directly from waveform segments without explicit peak detection [19]. However, PPG remains vulnerable to motion artifacts, which distort waveform morphology and compromise interval accuracy. To address this, prior work has proposed quality assessment-based segment rejection [25], or waveform restoration using deep architectures such as U-Net and LSTM [4, 15]. Some methods further incorporate reference signals (e.g., multi-wavelength PPG [4] or inertial data [17]) to aid waveform recovery.

While motion artifacts have been extensively studied, contact pressure is an underexplored yet distinct source of signal degradation. Hung et al. [11], for example, used a generative model to restore clean PPG signals degraded by poor contact, then computed HRV from the reconstructed waveform. In contrast, our method does not attempt to recover an ideal signal. We treat pressure as a discrete condition and directly estimate HRV from pressure-distorted segments. This bypasses both peak recovery and segment filtering, while enabling interpretable conditioning via a learned mapping from distorted waveforms to physiological variability.

7 DISCUSSION AND FUTURE WORK

Toward Demographically Robust Modeling. One limitation of our study lies in the demographic characteristics of the WF-PPG dataset [10]. All participants were healthy young adults (mean age 24.3 ± 2.74 years) without known cardiovascular or neurological conditions. As a result, their HRV values largely fall within the normal physiological range, limiting the diversity of cardiac dynamics captured by the dataset. This homogeneity may constrain the generalizability of our model to populations with atypical HRV patterns, such as elderly or patients with cardiovascular disorders.

In addition, age-related differences in skin and vascular properties may alter the way contact pressure affects PPG signals [31]. These mechanical and optical variations could lead to different distortion patterns not observed in our current dataset. Moreover, skin tone, which can influence light absorption and reflection [21], was not explicitly considered in our analysis but may affect signal quality and model performance. Future work should therefore include broader and more diverse populations in terms of age, skin type, and health status to evaluate model robustness under different physiological and biomechanical conditions.

Toward Broader Physiological Inference. While our study focuses on HRV estimation, PPG signals are also used to derive various other physiological indices, some of which may be even more sensitive to waveform distortions caused by contact pressure. These include blood pressure estimated from pulse morphology, often derived through intermediate indices such as pulse transit time and pulse wave velocity [27], as well as vascular aging markers like augmentation index and stiffness index [24]. Because all of these metrics depend on the fine structure of the PPG waveform—including features like the systolic peak, dicrotic notch, and wave valley—they are particularly susceptible to pressure-induced changes. Instead of aiming for general waveform recovery, our method explicitly incorporates contact pressure levels and focuses on directly estimating the physiological index of interest. This task-specific design enables more purposeful modeling and may yield greater accuracy for each physiological parameter of interest.

Toward Motion-Aware Pressure Modeling. Our current study focuses on static seated conditions, where contact pressure remains relatively stable. However, in real-world scenarios, particularly during physical activities such as walking or hand movements, contact pressure between the sensor and skin can also fluctuate significantly. For instance, rapid arm swings may cause a smartwatch to momentarily loosen or press more tightly against the wrist. While existing methods often rely on inertial measurements to correct motion-induced signal distortions [17], they typically overlook pressure variation as a contributing factor. Future work could explore combining IMU data with real-time pressure estimation to capture dynamic contact conditions and incorporate this information as an additional conditioning signal during physiological inference.

8 ACKNOWLEDGMENTS

This research was supported by the Singapore Ministry of Education (MOE) Academic Research Fund (AcRF) Tier 2 grant (Fund Code: T2EP20124-0046).

REFERENCES

[1] Malak Abdullah Almarshad, Md Saiful Islam, Saad Al-Ahmadi, and Ahmed S BaHammam. 2022. Diagnostic features and potential applications of PPG signal in healthcare: A systematic review. In *Healthcare*, Vol. 10. MDPI, 547.

[2] Roman M Baevsky and Anna G Chernikova. 2017. Heart rate variability analysis: physiological foundations and main methods. *Cardiometry* 10 (2017).

[3] Tanmoy Bhowmik, Jishnu Dey, and Vijay Narayan Tiwari. 2017. A novel method for accurate estimation of HRV from smartwatch PPG signals. In *2017 39th annual international conference of the IEEE engineering in medicine and biology society (EMBC)*. IEEE, 109–112.

[4] Marco Bolpagni, Sara Campanella, Silvia Gabrielli, and Lorenzo Palma. 2025. Segmentation of Motion Artifacts in Wearable PPG Signals Using Lightweight Neural Networks. *IEEE Sensors Journal* (2025).

[5] Nam Bui, Nhat Pham, Jessica Jacqueline Barnitz, Zhanan Zou, Phuc Nguyen, Hoang Truong, Taeho Kim, Nicholas Farrow, Anh Nguyen, Jianliang Xiao, et al. 2019. ebp: A wearable system for frequent and comfortable blood pressure monitoring from user's ear. In *The 25th annual international conference on mobile computing and networking*. 1–17.

[6] Yetong Cao, Huijie Chen, Fan Li, and Yu Wang. 2021. Crisp-BP: Continuous wrist PPG-based blood pressure measurement. In *Proceedings of the 27th Annual International Conference on Mobile Computing and Networking*. 378–391.

[7] Anand Chandrasekhar, Mohammad Yavarimanesh, Keerthana Natarajan, Jin-Oh Hahn, and Ramakrishna Mukkamala. 2020. PPG sensor contact pressure should be taken into account for cuff-less blood pressure measurement. *IEEE Transactions on Biomedical Engineering* 67, 11 (2020), 3134–3140.

[8] Xiang Chen, Tianjun Chen, Feifei Luo, and Jin Li. 2013. Comparison of valley-to-valley and peak-to-peak intervals from photoplethysmographic signals to obtain heart rate variability in the sitting position. In *2013 6th International Conference on Biomedical Engineering and Informatics*. IEEE, 214–218.

[9] Zhanjun Hao, Yifei Gao, Yangyang Tang, Yue Wang, Kai Fan, and Fenfang Li. 2025. FMCW-based contactless heart rate monitoring. *Scientific Reports* 15, 1 (2025), 2616.

[10] Matthew Yiwen Ho, Hung Manh Pham, Aaqib Saeed, and Dong Ma. 2025. WF-PPG: A wrist-finger dual-channel dataset for studying the impact of contact pressure on PPG morphology. *Scientific Data* 12, 1 (2025), 200.

[11] Manh Pham Hung, Matthew Yiwen Ho, Yiming Zhang, Dimitris Spathis, Aaqib Saeed, and Dong Ma. 2025. Reliable Physiological Monitoring on the Wrist Using Generative Deep Learning to Address Poor Skin-Sensor Contact. *arXiv preprint arXiv:2504.02735* (2025).

[12] Sinh Huynh, Rajesh Krishna Balan, JeongGil Ko, and Youngki Lee. 2019. VitaMon: measuring heart rate variability using smartphone front camera. In *Proceedings of the 17th Conference on Embedded Networked Sensor Systems*. 1–14.

[13] Hye-Geum Kim, Eun-Jin Cheon, Dai-Seg Bai, Young Hwan Lee, and Bon-Hoon Koo. 2018. Stress and heart rate variability: a meta-analysis and review of the literature. *Psychiatry investigation* 15, 3 (2018), 235.

[14] Ke Lu, Anna Sjörs Dahlman, Johan Karlsson, and Stefan Candefjord. 2022. Detecting driver fatigue using heart rate variability: A systematic review. *Accident Analysis & Prevention* 178 (2022), 106830.

[15] Akash Kumar Maity, Ashok Veeraraghavan, and Ashutosh Sabharwal. 2022. PPGMotion: Model-based detection of motion artifacts in photoplethysmography signals. *Biomedical Signal Processing and Control* 75 (2022), 103632.

[16] James M May, Elisa Mejía-Mejía, Michelle Nomoni, Karthik Budidha, Changmok Choi, and Panicos A Kyriacou. 2021. Effects of contact pressure in reflectance photoplethysmography in an in vitro tissue-vessel phantom. *Sensors* 21, 24 (2021), 8421.

[17] Philip Mehrgardt, Matloob Khushi, Simon Poon, and Anusha Withana. 2021. Deep learning fused wearable pressure and PPG data for accurate heart rate monitoring. *IEEE Sensors Journal* 21, 23 (2021), 27106–27115.

[18] Aditi Misra, Rohan Banerjee, Anirban Dutta Choudhury, Aniruddha Sinha, and Arpan Pal. 2015. Novel peak detection to estimate HRV using smartphone audio. In *2015 IEEE 12th International Conference on Wearable and Implantable Body Sensor Networks (BSN)*. IEEE, 1–6.

[19] Emad Kasaeyan Naeini, Fatemeh Sarhaddi, Iman Azimi, Pasi Liljeberg, Nikil Dutt, and Amir M Rahmani. 2023. A deep learning–based ppg quality assessment approach for heart rate and heart rate variability. *ACM Transactions on Computing for Healthcare* 4, 4 (2023), 1–22.

[20] Mimma Nardelli, Nicola Vanello, Guenda Galperti, Alberto Greco, and Enzo Pasquale Scilingo. 2020. Assessing the quality of heart rate variability estimated from wrist and finger ppg: A novel approach based on cross-mapping method. *Sensors* 20, 11 (2020), 3156.

[21] Ewa M Nowara, Daniel McDuff, and Ashok Veeraraghavan. 2020. A meta-analysis of the impact of skin tone and gender on non-contact photoplethysmography measurements. In *Proceedings of the IEEE/CVF Conference on Computer Vision and Pattern Recognition Workshops*. 284–285.

[22] Irene Pi, Isleen Pi, and Wei Wu. 2022. External factors that affect the photoplethysmography waveforms. *SN Applied Sciences* 4, 1 (2022), 21.

[23] Arvind Pillai, Dimitris Spathis, Fahim Kawsar, and Mohammad Malekzadeh. 2024. PaPaGei: Open Foundation Models for Optical Physiological Signals. *arXiv preprint arXiv:2410.20542* (2024).

[24] K Pilt, K Meigas, R Ferenets, K Temitski, and M Viigimaa. 2014. Photoplethysmographic signal waveform index for detection of increased arterial stiffness. *Physiological measurement* 35, 10 (2014), 2027.

[25] David Pollreisz and Nima TaheriNejad. 2022. Detection and removal of motion artifacts in PPG signals. *Mobile Networks and Applications* 27, 2 (2022), 728–738.

[26] Francesco Scardulla, Leonardo D'Acquisto, Raffaele Colombarini, Sijung Hu, Salvatore Pasta, and Diego Bellavia. 2020. A study on the effect of contact pressure during physical activity on photoplethysmographic heart rate measurements. *Sensors* 20, 18 (2020), 5052.

[27] Revati Shriram, Asmita Wakankar, Nivedita Daimiwal, and Dipali Ramdasi. 2010. Continuous cuffless blood pressure monitoring based on PTT. In *2010 International Conference on Bioinformatics and Biomedical Technology*. IEEE, 51–55.

[28] Jukka-Pekka Sirkiä, Tuukka Panula, and Matti Kaisti. 2024. Investigating the impact of contact pressure on photoplethysmograms. *Biomedical Engineering Advances* 7 (2024), 100123.

[29] Julian F Thayer, Shelby S Yamamoto, and Jos F Brosschot. 2010. The relationship of autonomic imbalance, heart rate variability and cardiovascular disease risk factors. *International journal of cardiology* 141, 2 (2010), 122–131.

[30] Simhadri Vadrevu and M Sabarimalai Manikandan. 2018. A robust pulse onset and peak detection method for automated PPG signal analysis system. *IEEE Transactions on Instrumentation and Measurement* 68, 3 (2018), 807–817.

[31] Q Yousef, MBI Reaz, and Mohd Alauddin Mohd Ali. 2012. The analysis of PPG morphology: investigating the effects of aging on arterial compliance. *Measurement Science Review* 12, 6 (2012), 266.